Freeze-Drying as a Novel Concentrating Method for Wastewater Detection of SARS-CoV-2

*Rui Dong[a], Elizabeth Noriega Landa[a], Hugues Ouellet[b], Wen-Yee Lee[a], Chuan Xiao[a]**

[a]Department of Chemistry and Biochemistry, The University of Texas at El Paso, 500 W. University Ave, El Paso, TX 79902, USA

[b]Department of Biological Sciences, The University of Texas at El Paso, 500 W. University Ave, El Paso, TX 79902, USA

Abstract

Detecting viral RNA from wastewater has emerged as a cost-effective approach for community-level surveillance during the recent SARS-CoV-2 pandemic. Although various concentrating methods have been developed, none are optimal for all key requirements for wastewater viral detection. Freeze-drying, a technique widely used for concentrating and preserving biological materials, remains underexplored for this purpose. This study compared the performance of freeze-drying and centrifugal ultrafiltration in terms of recovery efficiency, detection limit, and other key parameters. Early pandemic samples in this study, with extremely low viral concentrations, offered an ideal benchmark to assess their suitability for early-warning applications. Statistical analyses showed that freeze-drying achieved significantly higher recovery efficiency (0.338% ± 0.065% vs. 0.149% ± 0.046%), superior detection ratio (81.6% vs. 36.8%), and lower detection limit (0.06 vs. 0.36 copies/mL) compared to centrifugal ultrafiltration. To our knowledge, this is the first study to apply freeze-drying for wastewater-based viral detection. Despite its longer processing time, freeze-drying offers multiple advantages, including the elimination of pretreatment steps, a flexible workflow, reduced RNA degradation under cryogenic conditions, minimal pathogen exposure, lower labor demands, and less human interference during processing. These features position freeze-drying as a novel

alternative for wastewater-based viral surveillance, particularly for decision-making when establishing such systems.

Keywords: wastewater; viral RNA detection; SARS-CoV-2; concentrating; freeze-drying; centrifugal ultrafiltration.

Synopsis:

Freeze-drying is a new wastewater virus concentrating method that outperforms centrifugal ultrafiltration, providing a simpler, safer, and more sensitive approach for community surveillance.

---

* Corresponding Author. Tel.: +01-915-747-8657

Email Address: cxiao@utep.edu

1. Introduction

Coronavirus disease 2019 (COVID-19) is caused by the Severe Acute Respiratory Syndrome Coronavirus 2 (SARS-CoV-2), a positive-sense enveloped single-stranded RNA virus. The World Health Organization declared COVID-19 a global pandemic in March 2020. As of December 15, 2024, over 7 million deaths have been reported worldwide.[1,2] Timely detection and monitoring of the virus at the early stages of a pandemic are crucial to mitigate its spread, and wastewater surveillance has emerged as a recognized and effective approach. Notably, in March 2020, Medema et al. reported the first detection of SARS-CoV-2 RNA in wastewater in the Netherlands, preceding major outbreaks in various regions.[3-5] Quantifying SARS-CoV-2 RNA in sewage offers the possibility of developing an early warning system, providing valuable

insights into disease prevalence and allowing public health authorities more time to intervene. Thus, sensitive and cost-effective methods are essential for such applications.

Nevertheless, assessing viral load within wastewater presents challenges due to the variable composition of sewage. Wastewater comprises both liquid and solid phases, each of which may contain viral signals.[3] Moreover, the composition of wastewater is influenced by numerous factors, including local precipitation, drought conditions, temperature fluctuations, and water usage patterns.[4] Therefore, the concentration of viruses in wastewater can fluctuate widely. In addition, nucleases in the environment can potentially degrade nucleic acids, particularly RNA, representing another significant factor impacting the detectable viral RNA concentration in wastewater.[5] Considering all these variables, detecting minute quantities of specific pathogens in the complex matrix of wastewater represents a substantial challenge, necessitating a proper sample concentrating method to maximize the preservation of signal for subsequent detection.

To tackle these challenges, a concentrating method should be developed specifically to address the properties of wastewater. Given the very low viral load during early and late pandemic stages (**Figure 1a** shaded area), the recovery rate and detection limit are the most critical criteria for evaluating concentrating methods. An effective method must efficiently collect viruses from both liquid and solid phases while protecting viral genomic materials from degradation. The method should avoid (1) pretreatments such as prefiltration that could result in the loss of viruses associated with solid particles;[6,7] (2) addition of chemicals that may inhibit downstream detection.[8–10] Additionally, especially for RNA viruses, the approach should minimize degradation caused by ubiquitous environmental RNases.[11] For resource-limited facilities such as wastewater treatment plants, the concentrating method should be easy to establish without specialized personnel training and biosafety infrastructure. In addition, labor-intensive processes

should be minimized in the protocol for long-term surveillance applications.[12] Despite these needs, an optimal concentrating method that effectively addresses all challenges for wastewater viral surveillance has not yet been established.

The U.S. Centers for Disease Control and Prevention (CDC) has outlined five methodologies for concentrating viral particles from wastewater including (1) centrifugal ultrafiltration, (2) electronegative membrane filtration, (3) polyethylene glycol (PEG) precipitation, (4) skimmed milk flocculation, and (5) ultracentrifugation.[13] While each of these methods employs different principles to address the challenges of low levels of viral RNA in wastewater,[6,14–19] none fully meets all the criteria for effectively concentrating and detecting viruses. Achieving sensitive viral RNA detection in wastewater samples, especially during the onset of COVID-19 outbreak with sporadic infections, necessitates the development of improved and more robust sample concentrating methods, as existing approaches often involve trade-offs between recovery efficiency, detection sensitivity, and operational complexity.

In contrast, freeze-drying, which is not listed by the CDC, is a promising alternative concentrating method that is widely used to preserve various biological products.[20,21] Recently, it has been applied to concentrate wastewater samples to evaluate the deactivation effect of Fe^{3+} treatment on bacteria,[22] yet its potential for wastewater-based virus detection has not been explored. Freeze-drying effectively removes water from wastewater matrices by sublimation. This method uniquely retains viral entities from both the liquid and solid components of wastewater, thereby enhancing detection sensitivity. Additionally, freeze-drying does not rely on reagent-dependent sample pre-treatment, thus preserving sample integrity without chemical interventions. The cryogenic environment during freeze-drying prevents the degradation of viral RNA, thereby improving the detection limit in the subsequent analyses. Although it is time-

consuming to process large-volume samples, freeze-drying offers operational convenience by minimizing human oversight after initial setup. In summary, freeze-drying may represent a novel and potentially sensitive alternative method for virus detection in wastewater, as it minimizes viral loss and optimizes the protection of viral RNA. Nevertheless, its effectiveness must be assessed by comparison with existing methods.

Here we report the first application of freeze-drying to measure SARS-CoV-2 levels in wastewater. A comparative analysis was conducted between freeze-drying and the widely used centrifugal ultrafiltration as concentrating methods for wastewater samples. Throughout the subsequent sections, “ultrafiltration” will be used in lieu of the more descriptive term "centrifugal ultrafiltration" to improve conciseness. Ultrafiltration was chosen for comparison because it is among the most widely used concentrating methods for SARS-CoV-2 in wastewater and has been employed in the first[23] and several early reports of wastewater-based surveillance[24–26]. In addition, comparative studies have demonstrated that ultrafiltration frequently achieves virus recovery efficiencies and detection sensitivities matching or exceeding those of other concentrating methods such as precipitation or flocculation, particularly at low viral loads.[12,27–29] Given this widespread adoption and the consistently strong performance documented across multiple studies, ultrafiltration represents an appropriate benchmark against which to assess the advantages and limitations of the freeze-drying approach. Critical factors, including recovery efficiency and detection limits, were systematically compared and evaluated using RT-qPCR across both concentrating methods.

The wastewater samples tested in this study are of exceptional value because they were collected during the critical onset and waning phases of pandemic peaks (**Figure 1a**). During these periods, viral concentrations were extremely low, highlighting the value of this comparison in selecting a better concentrating method for establishing a wastewater-based early warning system. Before using these precious samples, thorough method testing and optimization were carried out using DNA and RNA standards, as well as a similar but less pathogenic coronavirus. Although each invaluable sample could be processed only once by each concentrating method due to limited sample volume, our optimized utilization strategy ensured reliable quantitative measurements while maximizing meaningful insights from these irreplaceable specimens. The resulting data provides important evidence supporting freeze-drying as a promising and innovative alternative concentrating method to detect viruses in wastewater. These findings can inform decision-making during the establishment and optimization of such monitoring systems and ultimately enhancing community-level early warning and wastewater surveillance capabilities.

2. Material and Methods

2.1. Sample Collection and Pretreatments

A total of 82 influent wastewater samples, each composited over 24 h, were collected on designated dates, from February 17, 2020, to May 28, 2021, primarily during the early stages of the first COVID-19 pandemic peak in El Paso, Texas, USA, with additional samples collected during the low and steady tail of the first outbreak (**Figure 1a** grey shaded areas**, Table S6**). The wastewater samples were collected from four wastewater treatment plants (WWTPs) in El Paso, Texas, USA. These WWTPs were Haskell Street Wastewater Plant (HS), John T. Hickerson

134 Water Reclamation Facility (JH), Fred Hervey Water Reclamation (FH), and Roberto R.
135 Bustamante Wastewater Plant (BU). The locations of these WWTPs are shown in **Figure 1c**.
136 Due to safety concerns during the early phase of the pandemic (March 2020 to July 2020),
137 before the person-to-person transmission pathway of the SARS-CoV-2 was fully elucidated, a
138 sample collecting protocol was developed and approved by the Institutional Biosafety
139 Committee (IBC) of the University of Texas at El Paso (UTEP). Individuals collecting samples
140 wore double-layer disposable nitrile gloves, splash goggles, N95 or surgical masks, and
141 disposable lab coats as a precautionary measure. The designs of our wastewater sample
142 collection and processing protocols in the following sections reflect a strong commitment to high
143 safety standards in adhering to the stringent biosafety standards set by institutions such as the
144 CDC and NIH for emerging unknown pathogens. This proactive approach to biosafety was
145 crucial during uncertain times. Nevertheless, these precautionary sample collection protocols
146 may also be applicable for future emerging viruses.
147 Due to limited storage space in −80 °C freezers, a maximum of approximately 500 mL of
148 wastewater could be collected for each sampling event, and each sample was split into two ~200
149 mL portions, which were analyzed in parallel by the two concentrating methods: freeze-drying
150 and ultrafiltration (**Figure 1b**). During the early period from February to August 2020, 68
151 samples were collected and stored at −80 °C using the IBC-approved biosafety protocol
152 developed at UTEP, prior to finalization and IBC approval of the analytical protocol at the end of
153 2020. Some samples from certain WWTPs were unavailable due to technical and personnel
154 challenges encountered during the pandemic.
155 Due to the limited lab accessibility during the pandemic, human resource constraints, and the
156 restricted storage space in −80 °C freezers, sample collection was paused between August 2020

157 and April 2021. After samples were processed using the fully IBC-approved protocol, freeing
158 storage space in −80 °C freezers, sample collection resumed in May 2021. The collection
159 frequency during the second period was more sporadic, depending on the processing speed of
160 samples stored. For the second period, a total of 14 samples were collected.

161 Samples were collected in pre-cleaned, wide-mouth, sterile leak-proof bottles (Fisherbrand™,
162 Cat# 05719709), transported in double Ziploc bags within hard-plastic coolers to the biosafety
163 level 2 (BSL-2) lab, and handled under standard biosafety and disinfection procedures. For early
164 pandemic samples, from April 2020 to September 2020, bottles were immediately frozen and
165 stored at −80 °C. Later, after CDC published its guideline in September 2020 to inactivate
166 pathogens for wastewater virus detection,[30] samples collected after September 2020 were
167 pasteurized in a water bath at 65 °C for 90 min before being stored at −80 °C. For those early
168 samples without pasteurization, before processing, they were thawed and pasteurized as
169 recommended by CDC guidelines. Following pasteurization, 82 samples were concentrated using
170 freeze-drying and 81 using ultrafiltration, respectively.

171

172

173

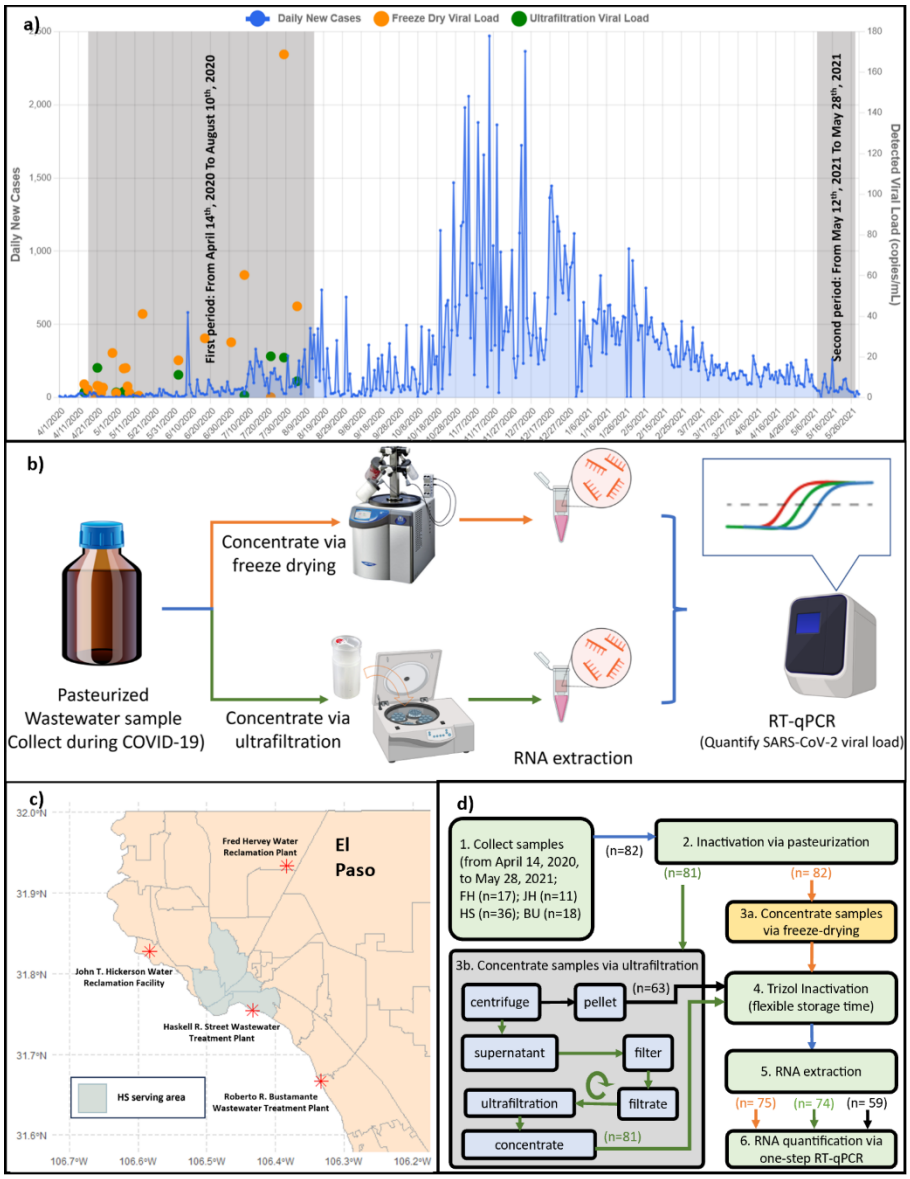
a)
Daily New Cases
Freeze Dry Viral Load
Ultrafiltration Viral Load
Daily New Cases
Detected Viral Load (copies/mL)
First period: From April 14th, 2020 To August 10th, 2020
Second period: From May 12th, 2021 To May 28th, 2021
b)
Pasteurized Wastewater sample Collect during COVID-19)
Concentrate via freeze drying
Concentrate via ultrafiltration
RNA extraction
RT-qPCR
(Quantify SARS-CoV-2 viral load)
c)
El Paso
Fred Hervey Water Reclamation Plant
John T. Hickerson Water Reclamation Facility
Haskell R. Street Wastewater Treatment Plant
Roberto R. Bustamante Wastewater Treatment Plant
HS serving area
d)
1. Collect samples (from April 14, 2020, to May 28, 2021; FH (n=17); JH (n=11) HS (n=36); BU (n=18)
(n=82)
2. Inactivation via pasteurization
(n=81)
(n= 82)
3a. Concentrate samples via freeze-drying
3b. Concentrate samples via ultrafiltration
centrifuge
pellet
(n=63)
supernatant
filter
ultrafiltration
filtrate
concentrate
(n=81)
4. Trizol Inactivation (flexible storage time)
5. RNA extraction
(n= 75)
(n= 74)
(n= 59)
6. RNA quantification via one-step RT-qPCR

174

175 **Figure 1. Experimental design. (a)** El Paso COVID-19 pandemic data: daily new case numbers (blue line, left y-
176 axis) plotted alongside detected viral loads (right y-axis, copies/mL) determined by freeze-drying (orange dots) and
177 ultrafiltration (green dots). The two sample collection periods are shaded in grey. **(b)** Comparison workflow of
178 concentrating methods: parallel workflow comparing freeze-drying (orange lines) versus ultrafiltration (green lines)
179 as concentrating methods for wastewater virus detection. **(c)** Locations of wastewater treatment plants (WWTPs) in
180 El Paso: four El Paso WWTPs marked with red "*" symbols and labeled on the map. The El Paso area is shown in
181 pale orange, with the area served by HS shaded in grey. **(d)** Sample processing workflow and numbers: samples
182 collected from four different WWTPs were inactivated through pasteurization and then concentrated using two
183 methods (orange lines for freeze-drying, green lines for ultrafiltration, and black lines for pellets from the pre-
184 clarification step of ultrafiltration) . FH, Fred Hervey Water Reclamation Plant; JH, John T. Hickerson Water
185 Reclamation Facility; HS, Haskell R. Street Wastewater Treatment Plant; BU, Roberto R. Bustamante Wastewater
186 Treatment Plant. The number (n) of samples processed at each step is indicated in parentheses.

187 ## 2.2. Wastewater Sample Concentrating via Freeze-drying

188 Although samples were pasteurized and thus considered to be BSL-1 according to the CDC
189 guidelines,[30] a fully sealed freeze-drying setup was cautiously designed and implemented using a
190 FreeZone 2.5 Liter −84 °C Benchtop Freeze Dryer (Labconco™, Cat# 710201000). This design
191 is illustrated in **Figure 2**. The biosafety setup incorporated multiple safeguards: (1) The freeze
192 dryer vacuum chamber contained PTFE-coated coil, which is resistant to erosive disinfectants
193 used after each freeze-drying cycle; (2) Three layers of Filter papers (Labconco™, Cat#
194 7544810) and an aseptic valve (Labconco™, Cat# 7543900) were added between the fast-freeze
195 flask and manifold to prevent any potential accidental pathogen from passing through the
196 system; (3) A HEPA filter was added before the vacuum pump as the last filter to capture any
197 potential accidental pathogen leakage and spillage; (4) Wastewater samples were placed inside
198 plastic containers which were wrapped with absorbent pads in Fast-Freeze Flasks. The absorbent
199 pads were intended to capture any accidental spills; and (5) The exhaust pipe of the vacuum

200 pump was connected to a chemical fume hood, to exhaust odorous volatile organic compounds
201 from the wastewater. Even with these safety designs, as an additional precaution, all potentially
202 contaminated containers and the flow path before the HEPA filter were disinfected after each
203 freeze-drying run.

204 Systematically varied parameters such as sample volume, sample container (flask or bottle),
205 wrapping or no wrapping, distance between the sample container and freeze-drying flask, the
206 type of freeze-drying flask, and freeze-drying time were tested over several months before
207 optimized freeze-drying conditions were established as described below.

208 As shown in **Figure 1b and d**, prior to the freeze-drying procedure, approximately 200 mL of
209 each pasteurized wastewater sample from **Section 2.1** was weighed and aliquoted into a 250 mL
210 sterile plastic storage bottle (Thermo Scientific, Cat# 4550250), wrapped with absorbent pads,
211 placed into a Ziploc bag, and frozen at −80 °C at least one night.

212 On the day of concentrating, the frozen samples in storage bottles wrapped with absorbent pads
213 were then placed in 600 mL Complete Fast-Freeze Flasks (Labconco™, Cat# 7540800) with
214 storage bottle caps loosened on top of plastic spacer (three caps from 50 mL conical tubes)
215 (**Figure 2**). Freeze-drying was performed at −86 °C and 0.040 mbar. After approximately three
216 days, sample masses were reduced to about 3 g, with a small amount of ice remaining visible.
217 Complete desiccation was not pursued, as it would substantially increase processing time and
218 make the dried material more difficult to resolubilize in the subsequent step. Volume reduction
219 factors were estimated from sample weights measured before and after freeze-drying.

220 The freeze-dried samples were dissolved in three volumes (v/w; ~9 mL) of TRIzol™ LS
221 reagent (Thermo Fisher Scientific, Cat# 10296-028). Samples were vortexed to ensure thorough
222 mixing before storing at −20 °C until viral RNA extraction. It has been proven that TRIzol

223 deactivates all viral pathogens such as SARS-CoV-2 in the sample.[31] Therefore, the following
224 steps were considered as BSL-1.
225

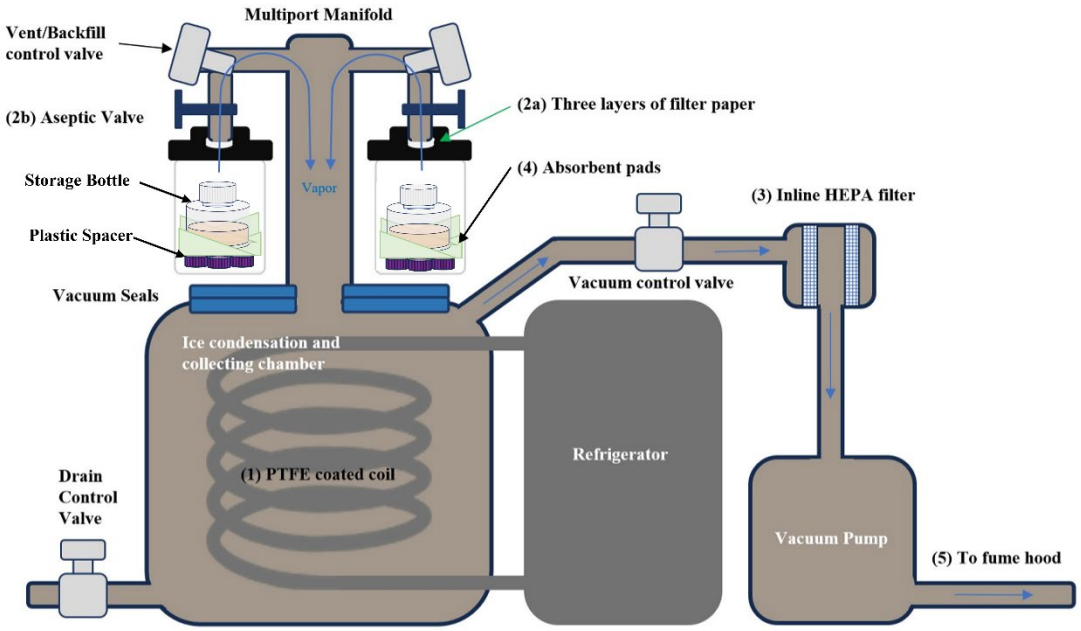

226

227 **Figure 2. Freeze-drying setup with biosafety safeguards.** Key biosafety safeguard features are
228 highlighted and labeled with numbers in the diagram.

229 ## 2.3. Sample Concentrating via Ultrafiltration

230 In parallel with concentrating samples via freeze-drying, another ~200 mL of pasteurized
231 wastewater sample from **Section 2.1** was aliquoted into four 50 mL conical tubes and loaded into
232 swinging buckets (Thermo Fisher Scientific, Cat# 75003655) with adaptors (Thermo Fisher
233 Scientific, Cat# 75003683) for the TX-400 rotor (Thermo Fisher Scientific, Cat# 75003181). The
234 swinging buckets were balanced and sealed with ClickSeal Biocontainment Lids (Thermo Fisher
235 Scientific, Cat# 75003656) and wiped with disinfectant on the outside before centrifuging at
236 3,000 × *g* for 15 min using Multifuge X1R Refrigerated Centrifuge (Thermo Fisher Scientific,

237 Cat# 75004251). After centrifugation, the supernatant was filtered using a 0.22 μm PES bottle
238 filter (Corning™, Cat# 431096) while the pellets were collected and weighed. In total, 63 pellets
239 were collected from 70 ultrafiltration samples (**Figure 1d**). Three volumes of TRIzol™ LS
240 reagent relative to the measured pellet weight were added to the pellet. TRIzol treated pellets
241 were vortexed to ensure thorough mixing before being stored at −20 °C until viral RNA
242 extraction to assess whether viral signals were associated with the solid phase. All these
243 procedures were carried out in a biosafety cabinet (BSC) to ensure safety. **Figure S1** illustrates
244 the filter system with multiple, precautionary safeguards: (1) A trap bottle with disinfectant at the
245 bottom was connected to the filter bottle to capture any potential accidental pathogen leakage
246 and spillage; (2) An in-line 0.22 μm filter was added before the vacuum valve to capture any
247 potential accidental pathogen leakage and spillage.

248 Inside the BSC, the filtered supernatants from the previous step were aliquoted (approximately
249 70 mL) into ultrafiltration units. In this study, Centricon Plus-70 with 10 kDa MW cutoff
250 membrane (MilliporeSigma, Cat# UFC701008 for 10 kDa) were used for most wastewater
251 samples. Two Centricon Plus-70 units with a 100 kDa cutoff membrane (MilliporeSigma, Cat#
252 UFC71008 for 100 kDa) and four 15 mL Amicon Ultra Centrifugal Filter with a 10 kDa cutoff
253 membrane (MilliporeSigma, Cat# UFC901024) were used in spiked recovery experiments to
254 evaluate the impact of different filter types. These concentrators were then placed into
255 disinfected swinging buckets (Thermo Fisher Scientific, Cat# 75003655, with seal cap Cat#
256 75003656). The buckets were carefully balanced and completely sealed with ClickSeal
257 Biocontainment Lids (Thermo Fisher Scientific, Cat# 75003656) and wiped with disinfectant on
258 the outside before being taken out of the BSC for loading onto the TX-400 rotor (Thermo Fisher
259 Scientific, Cat# 75003181).

260 The samples were centrifuged at 3,500 × *g* for approximately 15 min using Multifuge X1R
261 Refrigerated Centrifuge (Thermo Fisher Scientific, Cat# 75004251). After centrifugation, the
262 swinging buckets were taken back into the BSC, and the passthrough liquid was disinfected and
263 discarded. Following the same centrifugation protocol, the remaining filtered supernatants were
264 added to Centricon units and carefully balanced for the next round of concentrating via
265 ultrafiltration.

266 After three to four rounds of centrifugation, depending on wastewater viscosity and matrix
267 composition (e.g., dissolved high-molecular-weight organics and residual colloids), the sample
268 volume was reduced from 200 mL to approximately 0.5 mL. Following the manufacturer's
269 instructions, the Centricon Plus-70 filters were inverted and centrifuged at 1,000 × *g* to collect
270 the concentrates. The concentrated samples were subsequently transferred to new tubes and
271 mixed with three volumes (~1.5 mL) of TRIzol™ LS reagent. TRIzol treated samples were
272 vortexed to ensure thorough mixing before being stored at −20 °C until viral RNA extraction.
273 Volume reduction factors for ultrafiltration were determined by comparing the weights of the
274 samples before and after concentrating. All the filters and liquid transfer pipettes were soaked in
275 ~1% bleach for at least 15 min before being safely discarded.

276 **2.4. Primer–Probe Selection and Standard Curve Development**

277 As suggested by the CDC, SARS-CoV-2 RNA was quantified by one-step RT–qPCR using N1
278 and N2 primer-probe sets (**Table S1**) purchased from IDT (Cat# 10006713).[32] The performance
279 and efficiency of N1 and N2 primer-probe sets in the RT-qPCR assay were first evaluated by
280 generating standard curves using 10-fold serial dilutions (1 to 10^5 copies per reaction) of
281 templates: (1) a DNA plasmid containing the complete nucleocapsid gene of SARS-CoV-2 (IDT,

282 Cat# 10006625), and (2) Twist synthetic SARS-CoV-2 RNA (Twist Bioscience, Cat#
283 MT0075s44) with stock concentration of 2.0×10^5 copies/μL and 1.0×10^6 copies/μL, respectively.
284 Each diluted standard was aliquoted in triplicate and analyzed using the TaqPath™ 1-Step RT-
285 qPCR Master Mix (Thermo Fisher Scientific, Cat# A15299) in 20 μL reactions containing 5 μL
286 template, with primer and probe concentrations listed in **Table S1**. Triplicate water samples were
287 included as the negative controls. The one step RT-qPCR reactions were run at 50 °C for 15 min
288 and 95 °C for 2 min, followed by 45 cycles of 95 °C for 5 s and 55 °C for 30 s, per the
289 manufacturer's recommendations.
290 Standard curves were generated by least-squares regression of technical replicate data points,
291 and the fitting quality (R^2) and assay efficiency (E) were evaluated (**Figure S2; Table S2**). To
292 test template stability, standard curves were also generated after storing of standards at −20 °C
293 for up to four months. After evaluation (**Section S3; Section 3.1**), the N1 primer-probe set with
294 the DNA standard was selected to quantify all extracted RNA from wastewater samples.
295

296 **2.5. Viral RNA Extraction and Quantification**

297 SARS-CoV-2 RNA was extracted from the concentrated samples and purified using the
298 PureLink™ RNA Mini Kit (Thermo Fisher Scientific, Cat# 12183018A). Prior to RNA
299 extraction, the frozen samples mixed with TRIzol were thawed at room temperature. For every
300 milliliter of sample mixed with TRIzol, 0.2 mL Chloroform was added. The mixture was then
301 centrifuged at 12,000 × *g* at 4 °C for 15 min using a Microfuge 20R (Beckman Coulter, Cat#
302 B30148). Following centrifugation, the colorless upper aqueous phase, which contains the RNA,
303 was carefully extracted according to the manufacturer's instructions. The bound RNA was eluted
304 from the spin cartridge in 30 μL of ribonuclease-free water and collected by centrifugation. To

305 maximize RNA recovery, a second elution was performed by adding 100 μL of ribonuclease-free
306 water and centrifuging. The purified viral RNA was either immediately analyzed by one-step
307 RT-qPCR or stored at −20 °C to minimize degradation, depending on thermocycler availability.
308 RT-qPCR assays for RNA extracted from the same sampling event but split and concentrated
309 in parallel using the two methods, were always performed in the same runs to ensure identical
310 post-extraction processing.
311 Each RNA elution from extraction was aliquoted in triplicate and analyzed under identical one-
312 step RT-qPCR conditions as the DNA standard using the N1 primer-probe set (**Section 2.4**).
313 Viral concentrations were calculated as described in **Section S4**. These values represent the virus
314 recovered by each concentrating method and therefore allow direct comparison of their analytical
315 sensitivity.
316 During method development, including primer-probe set and standard evaluations, a Magnetic
317 Induction Cycler (Bio Molecular Systems, Cat# 71-101; 48 individual-tube reactions) was used.
318 After optimization and standardization, a StepOnePlus™ Real-Time PCR System (Thermo
319 Fisher Scientific, Cat# 4376600; 96-well plate format) was employed using identical
320 thermocycling conditions for all of the wastewater samples. DNA standards were run on both
321 thermocyclers (**Figure S2c**), and sample quantification was based on the standard curve
322 generated on the same instrument. Unfortunately, RT-qPCR data for some samples were lost
323 due to an unexpected crash of the computer controlling the StepOnePlus™ Real-Time PCR
324 System. Ultimately, quantification data were obtained from 75 freeze-dried samples, 74
325 ultrafiltration samples, and 59 pellets collected during the pre-clarification step of ultrafiltration
326 (**Figure 1d; Table S6**).

327 The one-step RT-qPCR assay was programmed for 45 amplification cycles with Ct values up
328 to 42 considered positive based on consistent amplification in technical replicates. This practice
329 aligns with CDC peer-reviewed SARS-CoV-2 wastewater surveillance protocols using 45-cycle
330 RT-qPCR, which routinely accept late Ct values near the cycling limit as positive when
331 supported by replicate consistency[33] and used by literature.[34,35]
332

333 **2.6. Recovery Efficiency Determination Using Human Coronavirus OC43**

334 Human coronavirus OC43 was used as a surrogate virus to compare recovery efficiencies of
335 the two concentrating methods. Both OC43 and SARS-CoV-2 are beta-coronaviruses that infect
336 the human respiratory tract[36,37], but OC43 causes only mild disease and therefore can be handled
337 in laboratory recovery experiments with fewer biosafety concerns.[38,39]
338 A standard curve of heat-inactivated OC43 (ZeptoMetrix, Cat# 0810024CFHI) was generated
339 to estimate the amount of virus spiked into wastewater. The stock concentration was provided in
340 $TCID_{50}$/mL, an infectivity-based unit defined as the dilution required to infect 50% of cell
341 monolayers.[40] Although $TCID_{50}$ does not directly represent genome copy number, it remains
342 proportional to infectious virus abundance. Because the objective of this study was method
343 comparison rather than absolute RNA quantification, $TCID_{50}$ provided a consistent internal
344 reference and has been used in previous wastewater virus studies.[41–44] All standard curve
345 preparation and spiking experiments used the same OC43 stock, and recovery efficiency was
346 expressed as a unitless ratio, making $TCID_{50}$ appropriate for this framework.
347 An exact 100 μL aliquot of inactivated OC43 (5.0×10^5 $TCID_{50}$/mL) was serially diluted
348 tenfold using molecular-grade water. Dilutions were subjected to the same TRIzol treatment,
349 RNA extraction, and RT-qPCR procedures described previously, using an OC43-specific primer-

350 probe set[45] (**Table S1**). A standard curve was established by plotting Ct values against the
351 logarithm of OC43 concentration ($TCID_{50}$/mL). Although extraction efficiency from stock
352 dilutions is unlikely to be 100%, both spiked wastewater samples and OC43 standards underwent
353 identical extraction and purification procedures, allowing proportional comparison.

354 For recovery efficiency experiments, 5.0×10^3 (low) or 2.5×10^4 (high) $TCID_{50}$ of heat-
355 inactivated OC43 were spiked into 200 mL raw influent wastewater (10 µL or 50 µL of the stock
356 solution, respectively). A 1 mL aliquot of the spiked sample was immediately mixed with 3 mL
357 TRIzol LS reagent (F-1mL and U-1mL in **Table S3**). The remaining sample, along with two
358 additional unspiked 200 mL controls (F0 and U0), was concentrated using either freeze-drying or
359 ultrafiltration following the procedures described in **Sections 2.2** and **2.3**, and viral RNA was
360 quantified by RT-qPCR in technical triplicate (**Section 2.5**).

361 For low-dose experiments (**Figure 3**; **Table S3**), one sample for each concentrating method
362 was spiked after pasteurization (F4 and U4) to evaluate potential pasteurization effects. Three
363 freeze-drying samples (F5–F7) and four ultrafiltration samples (U5–U8) were spiked before
364 pasteurization. To examine the influence of filter type under low-dose conditions, ultrafiltration
365 samples used different filters: Centricon Plus-70 with 10 kDa cutoff (U5), Centricon Plus-70
366 with 100 kDa cutoff (U6 and U7), and four Amicon Ultra 15 mL centrifugal filters with 10 kDa
367 cutoff (U8).

368 For high-dose experiments, three independent wastewater samples (biological n = 3) were
369 spiked for each concentrating method (F1–F3 and U1–U3 in **Figure 3** and **Table S3**).
370 Ultrafiltration in these experiments used Centricon Plus-70 with a 10 kDa cutoff membrane.

371 Recovered virus concentrations were estimated from RT-qPCR Ct values and the OC43
372 standard curve, expressed as $TCID_{50}$/mL, and used to calculate total recovered virus based on

sample volumes. Recovery efficiency was defined as the ratio of recovered virus to the amount initially spiked (**Figure 3**; **Table S3**; **Table S4** for statistical analyses).

Recovery efficiencies were determined from at least three independent biological replicates ($n \geq 3$) per method, each analyzed in technical triplicate, allowing calculation of the mean and standard deviation. Molecular-grade water blanks confirmed the absence of contamination. A Wilcoxon rank-sum test, which does not assume normal distribution,[46–48] was used to evaluate statistical differences between the two concentrating methods. The statistical analyses were conducted with functions wilcox.test() from the stats (version 4.3.1) package in R Studio.[49]

2.7. Method-specific Detection Limits

Method-specific detection limits were operationally defined as the lowest non-zero SARS-CoV-2 concentration (copies/mL) detected among processed wastewater samples, reflecting practical sensitivity in complex matrices. This approach has been used in previous wastewater studies.[50,51] Method-specific detection limits are reported in the last row of **Table S6**. Additional spiking experiments using DNA standards at the estimated threshold were performed to partially verify the magnitude level of these limits (**Section S7; Table S5**). These values represent operational metrics for comparing workflow sensitivity rather than formal Minimum Information for Publication of Quantitative Real-Time PCR Experiments (MIQE)-compliant assay limits of detection (LODs).[52,53]

393 **2.8. COVID-19 Case Data and Statistical Analyses**

394 Daily COVID-19 records from April 14, 2020, to May 28, 2021, in El Paso, TX, were
395 collected from https://www.epstrong.org/results.php and
396 https://elpasocovid19tracker.com/index.html (accessed 2025-11-18) (**Figure 1a**). Viral load data
397 from Haskell Street Wastewater Plant (HS), which had the largest number of wastewater
398 samples, together with the corresponding daily COVID-19 case counts on the wastewater sample
399 collection dates were compiled and listed in **Table S7**. The areas from where the case numbers
400 were collected correspond to the regions served by HS, including zip codes 79901, 79902,
401 79903, 79905, and 79930 (**Figure 1c**).

402 The association between total COVID-19 cases and SARS-CoV-2 viral load in wastewater was
403 first tested for normality using the Shapiro–Wilk test.[54] The variables significantly deviated from
404 normality ($p < 0.05$). Because Pearson's correlation assumes normally distributed data,
405 Spearman's rank correlation (ρ), a nonparametric test that does not require normality, was
406 instead used to assess the relationship between the variables.[55] This correlation can be denoted as
407 rho "ρ", ranging from -1 to 1, provided a quantitative measure of the observed relationship
408 between the two variables: daily COVID-19 case numbers and SARS-CoV-2 viral load in
409 wastewater. A ρ close to zero indicates no correlation, while close to 1 and -1 indicates strong
410 positive or negative correlation, respectively. The data processing and statistical analyses were
411 conducted with functions shapiro.test(), cor.test(), and wilcox.test() from the stats (version 4.3.1)
412 package in R Studio.[49]

413

414 ## 3. Results and Discussion

415 ### 3.1. RT-qPCR Primer-Probe Set Selection and Template Stabilities

416 Based on the evaluation of primer–probe sets and DNA/RNA standards, the N1 primer-probe
417 set was selected as the optimal choice for RT-qPCR quantification of wastewater samples due to
418 its stronger linear correlation and superior amplification efficiency, whereas DNA standards
419 were chosen because of their greater stability (**Section S3**). While RNA standards are preferred
420 for absolute quantification of RNA viruses due to minor differences in RT-qPCR amplification
421 efficiency between DNA and RNA templates, synthetic RNA standards are costly, prone to
422 degradation, and less stable for long-term usage. DNA standards have been widely used in
423 SARS-CoV-2 wastewater studies[56,57] and were empirically validated in this study, which
424 focusing on comparing to different concentrating methods. Our primary conclusions regarding
425 relative method performance (recovery efficiency, detection ratio, and method-specific detection
426 limit) are unaffected by the choice of standard, as they are based on method-paired analyses in
427 which identical standards were applied to both freeze-drying and ultrafiltration workflows.

428 Based on the observed degradation of RNA standards (**Section S3, Figure S2**), specific
429 precautions must be followed to mitigate RNA degradation in concentrated wastewater and
430 preserve its integrity for potential future analyses. Immediate sample processing after collection
431 is ideal for maximizing RNA extraction yield and maintaining its integrity. However, logistical
432 constraints often necessitate sample storage, for which TRIzol™ or similar denaturing reagents
433 are highly recommended. TRIzol effectively inhibits RNase activity, thereby preventing RNA
434 degradation.[58] Concentrated samples in TRIzol demonstrate superior stability for long-term
435 storage, particularly when stored at −80 °C.[59] Thus, maintaining samples in TRIzol without RNA
436 extraction until imminent RT-qPCR analysis is considered the optimal storage strategy.

437 Moreover, minimizing freeze-thaw cycles of samples, regardless of the storage method, is
438 critical to prevent RNA degradation. RNases are prevalent and can regain enzymatic activity
439 once denaturing conditions are removed.[60] Consequently, after RNA is extracted from the TRIzol
440 storage solution, downstream procedures should be performed promptly to minimize RNA
441 degradation and ensure the reliability and accuracy of the subsequent RT-qPCR analyses.
442 It is important to acknowledge that logistical constraints during the study period led to some
443 variation in sample processing. Specifically, some samples were stored at −80 °C prior to
444 pasteurization, others were pasteurized and then stored, and some underwent immediate
445 pasteurization followed by extraction (**Section 2.1**). However, for each methodological
446 comparison between freeze-drying and ultrafiltration, paired samples were subjected to identical
447 pre- and post-concentrating steps. This internal consistency ensures that the observed differences
448 are attributable to the concentrating methods themselves.

449 **3.2. Comparison of Recovery Efficiency Between Two Concentrating Methods**

450 Recovery efficiencies (**Section 2.6** and **S5**) were 0.338% ± 0.065% for freeze-drying and
451 0.149% ± 0.046% for ultrafiltration at a high spike level (2.5×10^4 $TCID_{50}$ per 200 mL). At a
452 lower spike level (5×10^3 $TCID_{50}$ per 200 mL), efficiencies decreased to 0.123% ± 0.025% and
453 0.062% ± 0.011%, respectively. Freeze-drying showed significantly higher recovery than
454 ultrafiltration (Wilcoxon rank-sum test, $p = 5.7 \times 10^{-4}$ for the high dose and $p = 1.7 \times 10^{-5}$ for the
455 low dose) **(Table S4**).
456 The recovery efficiency observed in this study is lower than the ~25% reported by Ye et al.
457 using ultrafiltration,[29] likely due to the substantially higher spiking concentration in that study
458 (~3×10^4 PFU/mL). In contrast, our highest spiking condition corresponded to 125 $TCID_{50}$/mL,

459 equivalent to approximately 47–58 PFU/mL based on established theoretical61 and simulation62
460 relationships (0.56–0.69 PFU per $TCID_{50}$), representing a >500-fold lower input concentration.
461 Lower input concentrations are expected to yield reduced apparent recovery efficiencies due to
462 stochastic effects and increased influence of matrix-associated losses. Consistent with this
463 expectation, our two-level spiking experiments showed higher recovery efficiencies at higher
464 initial concentrations (**Figure S3; Table S4**).
465 Based on literature-reported relationships between genome copy number and $TCID_{50}$ for the
466 OC43 stock,[61] together with our measured recovery efficiency and RT-qPCR standard curves
467 (Figure S2; Table S3), the expected Ct value is approximately ~28, which is in reasonable
468 agreement with the observed values (**Table S3**). However, the ratio between infectivity-based
469 units and genome copy number is inherently variable and depends on virus preparation,
470 inactivation, and environmental conditions. Therefore, this conversion is used only as an
471 approximate scaling factor for consistency checks rather than as an absolute equivalence.
472 RNA extracted from independently spiked 1 mL samples without concentration (F-1mL and U-
473 1mL in **Table S3**) and from concentrated 200 mL unspiked wastewater samFples (F0 and U0 in
474 **Table S3**) showed no detectable Ct values within 45 cycles, indicating negligible endogenous
475 OC43 signals. Recovery efficiencies were not significantly affected by spiking before or after
476 pasteurization ($p = 0.27$ for freeze-drying; $p = 0.11$ for ultrafiltration, **Table S4**).
477 For ultrafiltration, four 15 mL Amicon Ultra filters yielded lower recovery than a single 70 mL
478 Centricon Plus-70 unit ($p = 0.004$), whereas membrane cutoff (10 kDa vs 100 kDa) had no
479 significant effect within 70 mL filters ($p = 0.47$) (**Table S4**). Accordingly, data from 15 mL
480 filters were excluded from ultrafiltration averages.
481

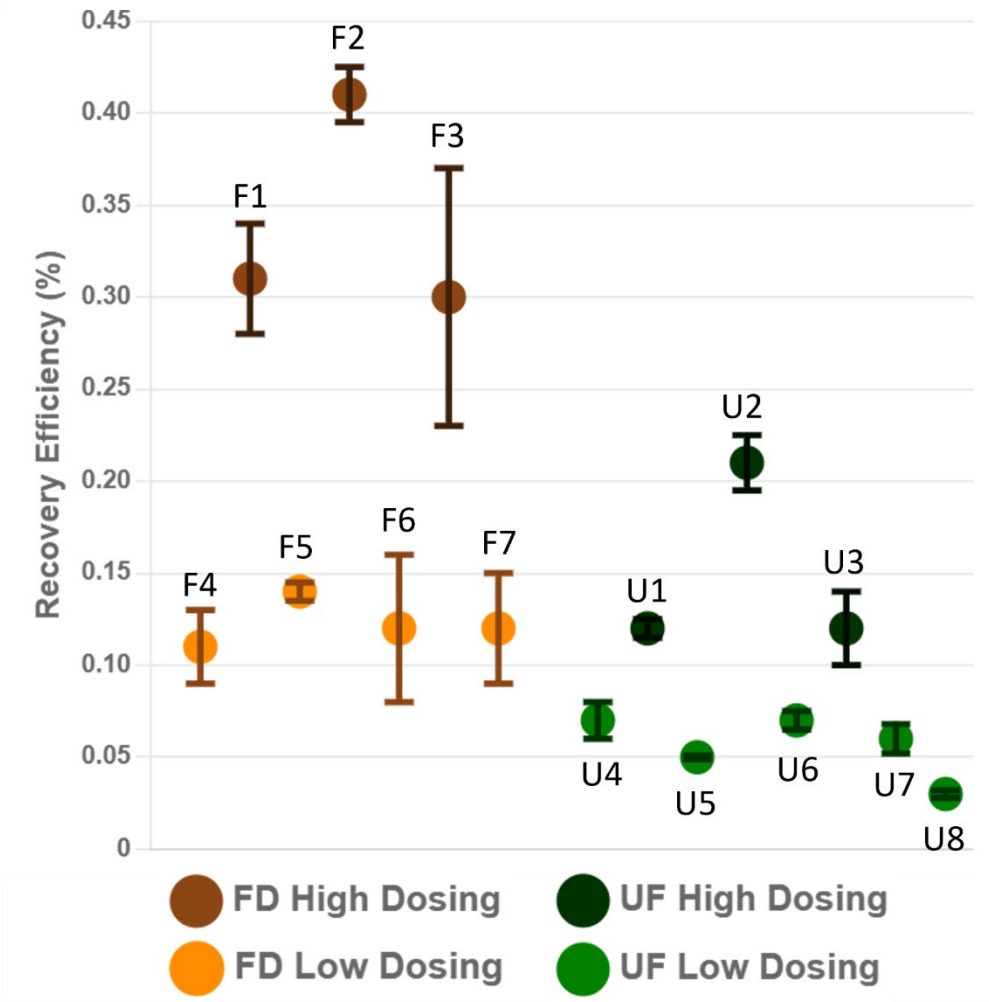

Figure 3. Recovery efficiency of the OC43 surrogate virus using freeze-drying and ultrafiltration concentrating methods. Heat-inactivated OC43 was spiked into influent wastewater samples, and recovery efficiencies were calculated based on RT-qPCR quantification of recovered viral RNA relative to the amount initially spiked. Sample IDs correspond to individual experimental replicates. Orange markers represent freeze-drying samples, and green markers represent ultrafiltration samples. Darker colors (F1–F3 and U1–U3) indicate higher spike levels, whereas the lighter-colored markers indicate lower spike levels. For selected samples, OC43 was added before pasteurization for most samples, except F4 and U4, which were spiked after pasteurization. For ultrafiltration samples, U1–U5 used 70 mL Centricon Plus-70 units with a 10 kDa cutoff membrane; U6 and U7 used 70 mL Centricon Plus-70 units with a 100 kDa cutoff membrane; and U8 used four 15 mL Amicon Ultra centrifugal filter units with a 10 kDa cutoff membrane. Error bars represent variability among technical RT-qPCR replicates.

3.3. Comparison of Early Detection of Two Concentrating Methods

The materials used in this study were precious and required careful stewardship. Prior to processing the pandemic-period samples, multiple trials using non-pandemic wastewater were conducted to optimize the workflow and quantification procedures. Due to the limited volumes collected during the early pandemic period, each invaluable sample could only be processed only once per concentrating method. However, triplicate RT-qPCR analyses were performed on RNA extracted from the concentrated samples, thereby maximizing the use of each collection and enabling reliable quantitative measurements despite constraints in sample availability, logistical challenges, and restricted laboratory access during pandemic-related shutdowns.

To evaluate the detection sensitivity of the freeze-drying and ultrafiltration methods, wastewater viral load data from the early onset phase of the COVID-19 pandemic (April to May 2020) were analyzed. A total of 38 samples were collected from wastewater treatment plants in El Paso, Texas, USA (**Table S6**, shaded rows), of which 33 had RT-qPCR data available. Using only the first elution, freeze-drying identified 31 positive samples (93.9%), whereas ultrafiltration detected 14 (42.4%). When the second elution was included, the detection rate for freeze-drying increased to 32 positives (97.0%), while ultrafiltration showed no increase (**Table 1**). The significantly higher detection rate observed with freeze-drying ($p = 1.01 \times 10^{-5}$ using only the first elution; $p = 1.36 \times 10^{-6}$ when second elutions were included, **Section S6**) highlights its superior ability to concentrate viral material compared with ultrafiltration. This advantage is particularly important for early warning systems for emerging virus surveillance.

517 **Table 1.** Positive detection rate and viral load for wastewater samples collected from four WWTPs between April
518 and May 2020

Site	Number of Sample	Number of Positive Sample				Average Viral Load (copies/mL)	
		Freeze-drying	Ultrafiltration	Freeze-drying	Ultrafiltration	Freeze-drying	Ultrafiltration
HS	16	14 (15)*	5	87.5 (93.8)*	31.3	8.35	1.45
JH	1	1	1	100.0	100.0	6.76	3.08
FH	6	6	5	100.0	83.5	7.54	1.68
BU	10	10	3	100.0	30.0	12.43	2.31
Total	33	31 (32)*	14	93.9 (97.0)*	42.4	$p=1.01 \times 10^{-5}$ (1.36×10^{-6})	

519 * Numbers in the parentheses are values obtained from additional positive samples when second elution was included.
520

521 ### 3.4. Comparison of Viral Concentration Detected via the Two Concentrating Methods

522 The superior detection sensitivity of the freeze-drying method was further supported by the
523 higher virus load obtained during RT-qPCR analyses. Across all four wastewater treatment
524 plants, the freeze-drying method consistently exhibited a higher amount of viral RNA compared
525 to ultrafiltration (**Table S6**). A Wilcoxon rank-sum test, a nonparametric test that compares two
526 independent groups without assumption of normal distribution,[46] was conducted to compare
527 virus loads in the original wastewater samples across all four facilities. As described in **Section**
528 **2.5** and **S4**, the total virus copies were estimated using the DNA standard curve and the Ct
529 values. For both freeze-dry and ultrafiltration methods, both first and second elutions were
530 combined to calculate the total RNA copies, which can then be calculated to the detected viral
531 load (copies/mL) in the original wastewater samples. Where a method or elution did not detect
532 the virus, it was recorded as zero copies. Across 74 paired samples, freeze-drying detected a
533 significantly higher median viral load (7.05 copies/mL [IQR 3.52-31.17]) than ultrafiltration
534 (1.19 copies/mL [IQR 0.00-5.49]) (**Table S6,** bottom rows) (Wilcoxon rank-sum test, $p = 2.39 \times$
535 10^{-9}).

536

537 **3.5. Comparison of Method-Specific Detection Limits of the Two Concentrating Methods**

538 Using the definition in **Section 2.7**, the freeze-drying method exhibited a lower method-
539 specific detection limit (0.06 copies/mL) than ultrafiltration (0.36 copies/mL) (**Table S6**, last
540 row). The corresponding Ct values (39.2 and 36.6) fall within the validated range of the standard
541 curve, supporting the validity of these measurements.

542 DNA standard spiking experiments yielded a detectable range of 40–80 copies per 200 mL
543 (**Section S7**, **Table S5**). Although this appears higher than the 12 copies per 200 mL (0.06
544 copies/mL) inferred from wastewater samples, this difference is expected given the low recovery
545 efficiencies observed in this study (0.4%–0.1%; **Table S3**). Accounting for recovery losses,
546 detection of 12 copies after concentration corresponds to approximately 3,000–12,000 copies in
547 the original sample, indicating that the apparent discrepancy arises from recovery constraints
548 rather than overestimation of sensitivity.

549 Such discrepancies are expected, as wastewater detection sensitivity is strongly influenced by
550 method-dependent recovery efficiency and can vary by several orders of magnitude across
551 workflows.[62] Importantly, the spiking experiments do not constitute a full MIQE-compliant
552 determination of assay LOD; rather, they provide partial verification of the order of magnitude of
553 the method-specific detection limits defined here.

554

555 **3.6. Matrix Associated Inhibitory Factors**

556 Among the 75 wastewater samples analyzed, 73 freeze-dried samples were positive in either
557 the first or second elution. Of these, 68 (93.1%) showed detectable viral signals in the second

558 elution, including 25 (34.3%) samples with lower Ct values than in the first elution; notably, 7 of
559 these were undetected in the first elution (**Table S6**). Similarly but slightly less, among the 47
560 positive samples out of 74 ultrafiltration samples, only 33 (70.2%) showed detectable viral
561 signals in the second elution, and 10 (21.3%) exhibited lower Ct values in the second elution
562 compared with the first; 5 of these were undetected in the first elution.

563 This phenomenon may occur because both concentrating methods can potentially co-
564 concentrate RT-qPCR inhibitors. Many of these inhibitory substances may be enriched in the
565 first elution, while the remaining inhibitors become further diluted in the second elution (100 μL
566 in the second elution vs 30 μL in the first), leading to similar or even lower Ct values. Because
567 the freeze-drying process concentrates all solutes, including those associated with the solid
568 phase, inhibitory substances that affect RT-qPCR may also be enriched to a greater extent than in
569 ultrafiltration.

570 Although freeze-drying showed a higher percentage of detectable viral signals in the second
571 elution, which could lead to greater underestimation of viral abundance compared with
572 ultrafiltration, our data consistently showed lower Ct values and higher detection ratios in freeze-
573 dried samples than in ultrafiltration samples. This indicates that any inhibitory effects were
574 insufficient to offset the gain in viral recovery.

575 Unfortunately, this potential inhibition phenomenon was recognized only after completion of
576 all RT-qPCR runs, and retrospective inhibition testing was not feasible due to limited remaining
577 sample volume. Nevertheless, systematic inhibition assessments and the incorporation of
578 inhibitor-removal steps[63] should be explored in future optimization of freeze-drying as a
579 wastewater virus concentration method.

3.7. Correlation Between Wastewater Viral Load and COVID-19 Case Numbers

The relationship between wastewater viral load and community COVID-19 cases was examined to assess the epidemiological relevance of the two concentrating methods. Viral loads calculated from samples processed by freeze-drying and ultrafiltration (**Table S7**) were analyzed separately against reported COVID-19 case numbers in El Paso, TX, USA.

Normalization of viral load to account for variations in human wastewater contribution is often recommended. Creatinine-based normalization was attempted using a commercial colorimetric assay (**Section S8**);[64,65] however, creatinine concentrations in the collected samples were consistently below the detection limit of the kit (**Table S6,** last column), preventing reliable normalization as seen in literature.[64] Therefore, subsequent analyses were conducted using unnormalized viral load data, and the results are presented only as supplemental observations rather than definitive epidemiological conclusions.

Shapiro–Wilk tests indicated that viral load and case data were not normally distributed ($p = 4.8 \times 10^{-7}$, 1.8 × 10-6, and 1.4×10^{-7}, for virus concentration detected by freeze-drying, those detected by ultrafiltration, and community COVID-19 case numbers, respectively),[54] and therefore Spearman rank correlation[55] was used to evaluate associations between wastewater viral load and daily reported COVID-19 cases. Active case numbers were unavailable during the early pandemic period (April–May 2020), so daily reported cases were used instead.

Correlation analysis showed a weak positive but non-significant relationship between viral load measured by freeze-drying and daily cases ($\rho = 0.209$, $p = 0.339$). Similarly, viral loads obtained by ultrafiltration showed a moderate but non-significant correlation with reported cases ($\rho = 0.379$, $p = 0.0746$). These results are broadly consistent with the variable correlations reported in previous wastewater surveillance studies.[23,66,67] However, interpretation is limited by the small

603 sample size and the lack of reliable normalization for human wastewater contribution and other
604 factors.[68]

605 **3.8. Initial Capital Investment and Operational Costs**

606 From the perspective of initial capital investment, a freeze-dryer is comparably priced to the
607 refrigerated centrifuge required for ultrafiltration. The freeze-dryer used in this study costs
608 approximately $14,000, whereas the centrifuge costs approximately $16,000. Freeze-drying
609 additionally requires an ultra-low temperature (ULT) freezer, even lower-cost undercounter
610 models (e.g., K2 Scientific, Cat. #K203ULT) are approximately $7,200. However, most
611 laboratories already maintain ULT freezers for biological sample preservation, reducing the need
612 for this additional investment. In terms of operational consumables, ultrafiltration requires
613 disposable filters such as the filter used mostly in this study (MilliporeSigma Cat. #UFC701008)
614 cost approximately $43 per sample, whereas the freeze-drying method uses only inexpensive
615 sample bottles (Thermo Scientific Cat. #4550250) costing approximately $2.4 per sample. All
616 equipment and consumable prices list above were obtained with an institutional educational
617 discount at the time of the study.
618

619 **3.9. Pretreatment**

620 Prior to concentrating, wastewater samples were pasteurized, a standard biosafety practice in
621 SARS-CoV-2 wastewater analysis to inactivate infectious virus. Some studies have reported that
622 pasteurization may enhance SARS-CoV-2 RNA detection by disrupting particulate matrices and
623 releasing particle-associated viral RNA.[69] However, pasteurization showed no significant effect
624 on recovery efficiency in our experiments (**Table S4**). Because paired samples processed by both

625 concentrating methods underwent identical pasteurization treatment, this step does not affect the
626 comparative conclusions of this study.

627 Incorporating immediate pasteurization after sample collection also allows workflows to
628 transition rapidly to BSL-1 conditions, which provides a practical strategy for handling unknown
629 or emerging pathogens such as during the early stages of the COVID-19 pandemic when
630 transmission pathways were not yet fully understood. This approach may be particularly useful
631 for laboratories with limited capacity to establish or maintain BSL-2 facilities, including those
632 affiliated with wastewater treatment plants.

633 Ultrafiltration requires pretreatment steps such as centrifugation and filtration to remove solids
634 and large aggregates, which may lead to the loss of viral RNA associated with sewage
635 sludge.[29,70] In a subset of samples, SARS-CoV-2 RNA was detected in pellets generated during
636 the initial clarification step, indicating that part of the viral signal remained associated with
637 solids typically discarded prior to ultrafiltration (**Table S6**). Similar observations have been
638 reported in previous studies, where excluding solids from wastewater samples reduced viral
639 detection rates.[71] Detection of viral RNA in these pellets also confirms that TRIzol-chloroform
640 extraction can recover viral RNA from solid fractions. Because freeze-drying concentrates both
641 liquid and solid phases, viral RNA associated with both fractions can be extracted together, while
642 insoluble solids are removed during the centrifugal phase-separation step of RNA extraction.

643 Freeze-drying also offers advantages for RNA preservation and workflow flexibility. After
644 pasteurization, samples are immediately frozen at −80 °C, and the concentrating process
645 proceeds under ultra-low temperatures, minimizing RNA degradation in environments where
646 RNases are ubiquitous. This improved preservation may also contribute to the higher recovery
647 efficiency and detection sensitivity observed for freeze-drying. In contrast, ultrafiltration

648 typically requires immediate processing after pasteurization to avoid additional freeze–thaw
649 cycles, limiting scheduling flexibility and increasing operational burden when laboratory
650 resources are constrained. Freeze-drying allows samples to remain stored at ultra-low
651 temperatures until processing, effectively decoupling sample collection from concentrating and
652 providing greater flexibility for routine surveillance workflows.
653

654 **3.10. Labor, Training, and Biosafety**

655 From an operational perspective, ultrafiltration involves multiple centrifugation, balancing, and
656 liquid-handling steps, requiring substantial operator training, particularly when handling
657 unknown or emerging pathogens. These procedures also prolong operator exposure to
658 wastewater and may increase the risk of pathogen transmission. For example, when the
659 transmission route of SARS-CoV-2 was not yet fully understood, our original IBC-approved
660 protocol classified wastewater processing as BSL-2+ conditions. Due to the potential for
661 generating aerosols, ultrafiltration required rigorous PPEs (double-layer disposable nitrile gloves,
662 face shields, closed-front gowns, and powered air-purifying respirators), along with extensive
663 decontamination during multi-step centrifugation. These requirements led to labor-intensive
664 workflows and limited throughput to approximately eight samples per day.
665 In contrast, although the freeze-drying method requires approximately three days to
666 concentrate eight 200 mL samples to a final volume of ~3 mL, it minimizes operator exposure.
667 Sample handling is limited to brief steps during initial setup (e.g., cap loosening and flask
668 mounting; **Figure 2**), after which the material remains sealed within a closed system equipped
669 with multiple safeguards (**Figure 2**, **Section 2.2**). Decontamination is required only upon process
670 completion. Moreover, freeze-drying involves substantially fewer liquid-handling steps, reducing

671 opportunities for sample loss, cross-contamination, and other sources of human-factor variability
672 throughout the concentrating process (**Section 2.2** and **2.3**).

673 **4. Conclusion**

674 In summary, using invaluable wastewater samples collected during the onset and waning
675 phases of the first COVID-19 pandemic, this study indicates that freeze-drying may provide
676 improved recovery and detection sensitivity compared with ultrafiltration under the conditions
677 examined. The uniqueness and timing of these early-pandemic samples provide a rare
678 opportunity to rigorously evaluate method performance under conditions of low and emerging
679 viral prevalence. Freeze-drying's higher recovery rates, detection ratios, and sensitivity for viral
680 RNA are particularly crucial during such early phases, when viral loads are low and reliable
681 detection is most challenging.

682 Freeze-drying's operational advantages, including increased scheduling flexibility, reduced
683 labor intensity, and minimized exposure risks, make it especially suitable for settings with
684 limited technical expertise, personnel capacity, and biosafety infrastructure. Although freeze-
685 drying requires a much longer processing time, the reduced need for continuous operator
686 supervision and the use of inexpensive consumables can offset the slightly higher initial capital
687 investment. This is particularly advantageous for newly established or developing laboratories
688 with limited trained personnel or without extensive biosafety infrastructure to support frequent
689 hands-on manipulation of pathogens.

690 This study represents a pivotal step in applying freeze-drying as a concentrating method for
691 wastewater virus surveillance. Further optimization and comprehensive characterization are
692 warranted, particularly in thoroughly evaluating the effects of pasteurization, mitigating matrix-
693 associated inhibitors,[10] developing approaches to normalize human contributions to

694 wastewater,[72] and systematic lead–lag time analysis.[73] While this study focused on viral
695 detection, future investigations should expand to other pathogens, including bacteria,[74,75]
696 fungi,[76,77] and protozoa.[78,79] Overall, our findings establish freeze-drying as a novel, sensitive,
697 sustainable, and labor-saving alternative for wastewater concentrating, with strong potential for
698 early warning and community-level surveillance of emerging pathogens.

ACKNOWLEDGMENT

During the preparation of this work, the author(s) utilized ChatGPT to only enhance readability and improve language. Following its use, the authors carefully reviewed and edited the content as necessary and took full responsibility for the final version of the publication. The authors would like to acknowledge Teresa T. Alcala and El Paso Water Laboratory personnel: Hugo Ruiz at John T. Hickerson Water Reclamation Facility, Martin L. Ortiz at Roberto Bustamante Wastewater Plant, Rick Dominguez at Haskell Street Wastewater Plant, Roberto Hernandez at Fred Hervey Water Reclamation, for their assistance during wastewater sample collection especially during the COVID-19 pandemic period. This work received funding from the College of Science, University of Texas at El Paso. The work has used instruments in the Border Biomedical Research Center (BBRC) that is supported by the National Institutes on Minority Health and Health Disparities (NIMHD) of the National Institutes of Health (NIH) under award number U54MD007592. Special thanks go to BBRC personnel Georgialina Rodriguez and Ana P. Betancourt who helped us use the instruments. RD and CX also received support from the National Institute of General Medical Sciences (NIGMS) of NIH under award number R01GM129525 and from the Welch Foundation under Grant Number AH-2126-20220331. WYL received support from NIGMS of NIH under the award number SC1CA245675. The content is solely the responsibility of the authors and does not necessarily represent the official views of the funding agencies.

REFERENCES

(1) World Health Organization. *Coronavirus Disease (COVID-19): Situation Report, 158*; World Health Organization, 2020. https://apps.who.int/iris/handle/10665/332858 (accessed 2022-02-14).

(2) CDC. *COVID Data Tracker*. Centers for Disease Control and Prevention. https://covid.cdc.gov/covid-data-tracker (accessed 2022-02-14).

(3) Roldan-Hernandez, L.; Boehm, A. B. Adsorption of Respiratory Syncytial Virus, Rhinovirus, SARS-CoV-2, and F+ Bacteriophage MS2 RNA onto Wastewater Solids from Raw Wastewater. *Environ. Sci. Technol.* **2023**, *57* (36), 13346–13355. https://doi.org/10.1021/acs.est.3c03376.

(4) Hughes, J.; Cowper-Heays, K.; Olesson, E.; Bell, R.; Stroombergen, A. Impacts and Implications of Climate Change on Wastewater Systems: A New Zealand Perspective. *Clim. Risk Manag.* **2021**, *31*, 100262. https://doi.org/10.1016/j.crm.2020.100262.

(5) Farkas, K.; Hillary, L. S.; Malham, S. K.; McDonald, J. E.; Jones, D. L. Wastewater and Public Health: The Potential of Wastewater Surveillance for Monitoring COVID-19. *Curr. Opin. Environ. Sci. Health* **2020**, *17*, 14–20. https://doi.org/10.1016/j.coesh.2020.06.001.

(6) Zheng, X.; Deng, Y.; Xu, X.; Li, S.; Zhang, Y.; Ding, J.; On, H. Y.; Lai, J. C. C.; In Yau, C.; Chin, A. W. H.; Poon, L. L. M.; Tun, H. M.; Zhang, T. Comparison of Virus Concentration Methods and RNA Extraction Methods for SARS-CoV-2 Wastewater Surveillance. *Sci. Total Environ.* **2022**, *824*, 153687. https://doi.org/10.1016/j.scitotenv.2022.153687.

(7) Banadaki, M. D.; Torabi, S.; Rockward, A.; Strike, W. D.; Noble, A.; Keck, J. W.; Berry, S. M. Simple SARS-CoV-2 Concentration Methods for Wastewater Surveillance in Low Resource Settings. *Sci. Total Environ.* **2024**, *912*, 168782. https://doi.org/10.1016/j.scitotenv.2023.168782.

(8) Zafeiriadou, A.; Nano, K.; Thomaidis, N. S.; Markou, A. Evaluation of PCR-Enhancing Approaches to Reduce Inhibition in Wastewater Samples and Enhance Viral Load Measurements. *Sci. Total Environ.* **2024**, *955*, 176768. https://doi.org/10.1016/j.scitotenv.2024.176768.

(9) Huge, B. J.; North, D.; Mousseau, C. B.; Bibby, K.; Dovichi, N. J.; Champion, M. M. Comparison of RT-dPCR and RT-qPCR and the Effects of Freeze–Thaw Cycle and Glycine Release Buffer for Wastewater SARS-CoV-2 Analysis. *Sci. Rep.* **2022**, *12* (1), 20641. https://doi.org/10.1038/s41598-022-25187-1.

(10) Ahmed, W.; Simpson, S. L.; Bertsch, P. M.; Bibby, K.; Bivins, A.; Blackall, L. L.; Bofill-Mas, S.; Bosch, A.; Brandão, J.; Choi, P. M.; Ciesielski, M.; Donner, E.; D'Souza, N.; Farnleitner, A. H.; Gerrity, D.; Gonzalez, R.; Griffith, J. F.; Gyawali, P.; Haas, C. N.; Hamilton, K. A.; Hapuarachchi, H. C.; Harwood, V. J.; Haque, R.; Jackson, G.; Khan, S. J.; Khan, W.; Kitajima, M.; Korajkic, A.; La Rosa, G.; Layton, B. A.; Lipp, E.; McLellan, S. L.; McMinn, B.; Medema, G.; Metcalfe, S.; Meijer, W. G.; Mueller, J. F.; Murphy, H.; Naughton, C. C.; Noble, R. T.; Payyappat, S.; Petterson, S.; Pitkänen, T.; Rajal, V. B.; Reyneke, B.; Roman, F. A.; Rose, J. B.; Rusiñol, M.; Sadowsky, M. J.; Sala-Comorera, L.; Setoh, Y. X.; Sherchan, S. P.; Sirikanchana, K.; Smith, W.; Steele, J. A.; Sabburg, R.; Symonds, E. M.; Thai, P.; Thomas, K. V.; Tynan, J.; Toze, S.; Thompson, J.; Whiteley, A. S.; Wong, J. C. C.; Sano, D.; Wuertz, S.; Xagoraraki, I.; Zhang, Q.; Zimmer-Faust, A. G.; Shanks, O. C. Minimizing Errors in RT-PCR Detection and Quantification of SARS-CoV-2

RNA for Wastewater Surveillance. *Sci. Total Environ.* **2022**, *805*, 149877. https://doi.org/10.1016/j.scitotenv.2021.149877.

(11) Sanchez-Quete, F.; Chiang, L.; Caldera Sequeira, F.; Goitom, E.; Tsitouras, A.; Maere, T.; Vanrolleghem, P. A.; Dorner, S.; Frigon, D.; Loeb, S. K. Suspended Solids and Optimal RNase Inhibitors Impact the Partitioning and Decay of SARS-CoV-2 in Wastewater. *ACS EST Water* **2024**, *4* (12), 5980–5988. https://doi.org/10.1021/acsestwater.4c01074.

(12) Juel, M. A. I.; Stark, N.; Nicolosi, B.; Lontai, J.; Lambirth, K.; Schlueter, J.; Gibas, C.; Munir, M. Performance Evaluation of Virus Concentration Methods for Implementing SARS-CoV-2 Wastewater Based Epidemiology Emphasizing Quick Data Turnaround. *Sci. Total Environ.* **2021**, *801*, 149656. https://doi.org/10.1016/j.scitotenv.2021.149656.

(13) Parkins, M. D.; Lee, B. E.; Acosta, N.; Bautista, M.; Hubert, C. R. J.; Hrudey, S. E.; Frankowski, K.; Pang, X.-L. Wastewater-Based Surveillance as a Tool for Public Health Action: SARS-CoV-2 and Beyond. *Clin. Microbiol. Rev. 37* (1), e00103-22. https://doi.org/10.1128/cmr.00103-22.

(14) Lu, D.; Huang, Z.; Luo, J.; Zhang, X.; Sha, S. Primary Concentration – The Critical Step in Implementing the Wastewater Based Epidemiology for the COVID-19 Pandemic: A Mini-Review. *Sci. Total Environ.* **2020**, *747*, 141245. https://doi.org/10.1016/j.scitotenv.2020.141245.

(15) Farkas, K.; Pellett, C.; Alex-Sanders, N.; Bridgman, M. T. P.; Corbishley, A.; Grimsley, J. M. S.; Kasprzyk-Hordern, B.; Kevill, J. L.; Pântea, I.; Richardson-O'Neill, I. S.; Lambert-Slosarska, K.; Woodhall, N.; Jones, D. L. Comparative Assessment of Filtration- and Precipitation-Based Methods for the Concentration of SARS-CoV-2 and Other Viruses from Wastewater. *Microbiol. Spectr.* **2022**, *10* (4), e01102-22. https://doi.org/10.1128/spectrum.01102-22.

(16) Anderson-Coughlin, B. L.; Shearer, A. E. H.; Omar, A. N.; Wommack, K. E.; Kniel, K. E. Recovery of SARS-CoV-2 from Wastewater Using Centrifugal Ultrafiltration. *Methods Protoc.* **2021**, *4* (2), 32. https://doi.org/10.3390/mps4020032.

(17) Sapula, S. A.; Whittall, J. J.; Pandopulos, A. J.; Gerber, C.; Venter, H. An Optimized and Robust PEG Precipitation Method for Detection of SARS-CoV-2 in Wastewater. *Sci. Total Environ.* **2021**, *785*, 147270. https://doi.org/10.1016/j.scitotenv.2021.147270.

(18) Philo, S. E.; Ong, A. Q. W.; Keim, E. K.; Swanstrom, R.; Kossik, A. L.; Zhou, N. A.; Beck, N. K.; Meschke, J. S. Development and Validation of the Skimmed Milk Pellet Extraction Protocol for SARS-CoV-2 Wastewater Surveillance. *Food Environ. Virol.* **2022**, *14* (4), 355–363. https://doi.org/10.1007/s12560-022-09512-5.

(19) Fonseca, M. S.; Machado, B. A. S.; Rolo, C. de A.; Hodel, K. V. S.; Almeida, E. dos S.; de Andrade, J. B. Evaluation of SARS-CoV-2 Concentrations in Wastewater and River Water Samples. *Case Stud. Chem. Environ. Eng.* **2022**, *6*, 100214. https://doi.org/10.1016/j.cscee.2022.100214.

(20) Bhatnagar, B. S.; Tchessalov, S.; Lewis, L. M.; Johnson, R. Freeze Drying of Biologics. In *Encyclopedia of Pharmaceutical Science and Technology, Six Volume Set (Print)*; CRC Press, 2013.

(21) Alves, D.; Sparrow, R.; Garnier, G. Rapidly Freeze-Dried Human Red Blood Cells for Pre-Transfusion Alloantibody Testing Reagents. *J. Biomed. Mater. Res. B Appl. Biomater.* **2021**, *109* (11), 1689–1697. https://doi.org/10.1002/jbm.b.34825.

(22) Qin, C.; Chen, C.; Shang, C.; Xia, K. Fe3+-Saturated Montmorillonite Effectively Deactivates Bacteria in Wastewater. *Sci. Total Environ.* **2018**, *622–623*, 88–95. https://doi.org/10.1016/j.scitotenv.2017.11.302.

(23) Medema, G.; Heijnen, L.; Elsinga, G.; Italiaander, R.; Brouwer, A. Presence of SARS-Coronavirus-2 RNA in Sewage and Correlation with Reported COVID-19 Prevalence in the Early Stage of the Epidemic in The Netherlands. *Environ. Sci. Technol. Lett.* **2020**, *7* (7), 511–516. https://doi.org/10.1021/acs.estlett.0c00357.

(24) Fontenele, R. S.; Kraberger, S.; Hadfield, J.; Driver, E. M.; Bowes, D.; Holland, L. A.; Faleye, T. O. C.; Adhikari, S.; Kumar, R.; Inchausti, R.; Holmes, W. K.; Deitrick, S.; Brown, P.; Duty, D.; Smith, T.; Bhatnagar, A.; Yeager, R. A.; Holm, R. H.; von Reitzenstein, N. H.; Wheeler, E.; Dixon, K.; Constantine, T.; Wilson, M. A.; Lim, E. S.; Jiang, X.; Halden, R. U.; Scotch, M.; Varsani, A. High-Throughput Sequencing of SARS-CoV-2 in Wastewater Provides Insights into Circulating Variants. *Water Res.* **2021**, *205*, 117710. https://doi.org/10.1016/j.watres.2021.117710.

(25) Gonçalves, J.; Koritnik, T.; Mioč, V.; Trkov, M.; Bolješič, M.; Berginc, N.; Prosenc, K.; Kotar, T.; Paragi, M. Detection of SARS-CoV-2 RNA in Hospital Wastewater from a Low COVID-19 Disease Prevalence Area. *Sci. Total Environ.* **2021**, *755*, 143226. https://doi.org/10.1016/j.scitotenv.2020.143226.

(26) Kazenelson, J.; Jefferson, T.; Rhodes, R. G.; Cahoon, L. B.; Frampton, A. R. Detection of SARS-CoV-2 RNA in Wastewater from an Enclosed College Campus Serves as an Early Warning Surveillance System. *PLOS ONE* **2023**, *18* (7), e0288808. https://doi.org/10.1371/journal.pone.0288808.

(27) Farkas, K.; Pellett, C.; Alex-Sanders, N.; Bridgman, M. T. P.; Corbishley, A.; Grimsley, J. M. S.; Kasprzyk-Hordern, B.; Kevill, J. L.; Pântea, I.; Richardson-O'Neill, I. S.; Lambert-Slosarska, K.; Woodhall, N.; Jones, D. L. Comparative Assessment of Filtration- and Precipitation-Based Methods for the Concentration of SARS-CoV-2 and Other Viruses from Wastewater. *Microbiol. Spectr. 10* (4), e01102-22. https://doi.org/10.1128/spectrum.01102-22.

(28) Othman, I.; Helmi, A.; Slama, I.; Hamdi, R.; Mastouri, M.; Aouni, M. Evaluation of Three Viral Concentration Methods for Detection and Quantification of SARS-CoV-2 in Wastewater. *J. Water Health* **2023**, *21* (3), 354–360. https://doi.org/10.2166/wh.2023.264.

(29) Ye, Y.; Ellenberg, R. M.; Graham, K. E.; Wigginton, K. R. Survivability, Partitioning, and Recovery of Enveloped Viruses in Untreated Municipal Wastewater. *Environ. Sci. Technol.* **2016**, *50* (10), 5077–5085. https://doi.org/10.1021/acs.est.6b00876.

(30) CDC. *Laboratory Biosafety Guidelines for working with SARS-CoV-2*. COVID-19. https://www.cdc.gov/covid/php/lab/index.html (accessed 2025-11-05).

(31) Patterson, E. I.; Prince, T.; Anderson, E. R.; Casas-Sanchez, A.; Smith, S. L.; Cansado-Utrilla, C.; Solomon, T.; Griffiths, M. J.; Acosta-Serrano, Á.; Turtle, L.; Hughes, G. L. Methods of Inactivation of SARS-CoV-2 for Downstream Biological Assays. *J. Infect. Dis.* **2020**, *222* (9), 1462–1467. https://doi.org/10.1093/infdis/jiaa507.

(32) Lu, X.; Wang, L.; Sakthivel, S. K.; Whitaker, B.; Murray, J.; Kamili, S.; Lynch, B.; Malapati, L.; Burke, S. A.; Harcourt, J.; Tamin, A.; Thornburg, N. J.; Villanueva, J. M.; Lindstrom, S. US CDC Real-Time Reverse Transcription PCR Panel for Detection of Severe Acute Respiratory Syndrome Coronavirus 2. *Emerg. Infect. Dis.* **2020**, *26* (8), 1654–1665. https://doi.org/10.3201/eid2608.201246.

(33) Saber, L. B.; Kennedy, S. S.; Yang, Y.; et al. Correlation of SARS-CoV-2 in Wastewater and Individual Testing Results in a Jail, Atlanta, Georgia, USA. *Emerg. Infect. Dis.* **2024**, *30* (13), 21–27. https://doi.org/10.3201/eid3013.230775.
(34) Navarro, A.; Gómez, L.; Sanseverino, I.; Niegowska, M.; Roka, E.; Pedraccini, R.; Vargha, M.; Lettieri, T. SARS-CoV-2 Detection in Wastewater Using Multiplex Quantitative PCR. *Sci. Total Environ.* **2021**, *797*, 148890. https://doi.org/10.1016/j.scitotenv.2021.148890.
(35) Diamanti, C.; Nousis, L.; Bozidis, P.; Koureas, M.; Kyritsi, M.; Markozannes, G.; Simantiris, N.; Panteli, E.; Koutsolioutsou, A.; Tsilidis, K.; Hadjichristodoulou, C.; Koutsotoli, A.; Christaki, E.; Alivertis, D.; Bartzokas, A.; Gartzonika, K.; Dovas, C.; Ntzani, E. Wastewater Surveillance of SARS-CoV-2: A Comparison of Two Concentration Methods. *Viruses* **2024**, *16* (9), 1398. https://doi.org/10.3390/v16091398.
(36) V'kovski, P.; Kratzel, A.; Steiner, S.; Stalder, H.; Thiel, V. Coronavirus Biology and Replication: Implications for SARS-CoV-2. *Nat. Rev. Microbiol.* **2021**, *19* (3), 155–170. https://doi.org/10.1038/s41579-020-00468-6.
(37) Su, S.; Wong, G.; Shi, W.; Liu, J.; Lai, A. C. K.; Zhou, J.; Liu, W.; Bi, Y.; Gao, G. F. Epidemiology, Genetic Recombination, and Pathogenesis of Coronaviruses. *Trends Microbiol.* **2016**, *24* (6), 490–502. https://doi.org/10.1016/j.tim.2016.03.003.
(38) Sizun, J.; Yu, M. W. N.; Talbot, P. J. Survival of Human Coronaviruses 229E and OC43 in Suspension and after Drying Onsurfaces: A Possible Source Ofhospital-Acquired Infections. *J. Hosp. Infect.* **2000**, *46* (1), 55–60. https://doi.org/10.1053/jhin.2000.0795.
(39) Leung, N. H. L.; Chu, D. K. W.; Shiu, E. Y. C.; Chan, K.-H.; McDevitt, J. J.; Hau, B. J. P.; Yen, H.-L.; Li, Y.; Ip, D. K. M.; Peiris, J. S. M.; Seto, W.-H.; Leung, G. M.; Milton, D. K.; Cowling, B. J. Respiratory Virus Shedding in Exhaled Breath and Efficacy of Face Masks. *Nat. Med.* **2020**, *26* (5), 676–680. https://doi.org/10.1038/s41591-020-0843-2.
(40) Lei, C.; Yang, J.; Hu, J.; Sun, X. On the Calculation of TCID50 for Quantitation of Virus Infectivity. *Virol. Sin.* **2020**, *36* (1), 141–144. https://doi.org/10.1007/s12250-020-00230-5.
(41) Philo, S. E.; Keim, E. K.; Swanstrom, R.; Ong, A. Q. W.; Burnor, E. A.; Kossik, A. L.; Harrison, J. C.; Demeke, B. A.; Zhou, N. A.; Beck, N. K.; Shirai, J. H.; Meschke, J. S. A Comparison of SARS-CoV-2 Wastewater Concentration Methods for Environmental Surveillance. *Sci. Total Environ.* **2021**, *760*, 144215. https://doi.org/10.1016/j.scitotenv.2020.144215.
(42) Ahmed, W.; Angel, N.; Edson, J.; Bibby, K.; Bivins, A.; O'Brien, J. W.; Choi, P. M.; Kitajima, M.; Simpson, S. L.; Li, J.; Tscharke, B.; Verhagen, R.; Smith, W. J. M.; Zaugg, J.; Dierens, L.; Hugenholtz, P.; Thomas, K. V.; Mueller, J. F. First Confirmed Detection of SARS-CoV-2 in Untreated Wastewater in Australia: A Proof of Concept for the Wastewater Surveillance of COVID-19 in the Community. *Sci. Total Environ.* **2020**, 138764. https://doi.org/10.1016/j.scitotenv.2020.138764.
(43) Dallner, M.; Harlow, J.; Nasheri, N. Efficacy of Washing Produce in Removing Human Coronavirus OC43 and Murine Norovirus. *J. Appl. Microbiol.* **2022**, *133* (3), 1800–1807. https://doi.org/10.1111/jam.15667.
(44) Fischer, R.; Judson, S.; Miazgowicz, K.; Bushmaker, T.; Prescott, J.; Munster, V. J. Ebola Virus Stability on Surfaces and in Fluids in Simulated Outbreak Environments. *Emerg. Infect. Dis.* **2015**, *21* (7), 1243–1246. https://doi.org/10.3201/eid2107.150253.
(45) Dare, R. K.; Fry, A. M.; Chittaganpitch, M.; Sawanpanyalert, P.; Olsen, S. J.; Erdman, D. D. Human Coronavirus Infections in Rural Thailand: A Comprehensive Study Using Real-

Time Reverse-Transcription Polymerase Chain Reaction Assays. *J. Infect. Dis.* **2007**, *196* (9), 1321–1328. https://doi.org/10.1086/521308.

(46) Ramachandran, K. M.; Tsokos, C. P. Chapter 12 - Nonparametric Tests. In *Mathematical Statistics with Applications in R (Second Edition)*; Ramachandran, K. M., Tsokos, C. P., Eds.; Academic Press: Boston, 2015; pp 589–637. https://doi.org/10.1016/B978-0-12-417113-8.00012-6.

(47) MacFarland, T. W.; Yates, J. M. Mann–Whitney U Test. In *Introduction to Nonparametric Statistics for the Biological Sciences Using R*; MacFarland, T. W., Yates, J. M., Eds.; Springer International Publishing: Cham, 2016; pp 103–132. https://doi.org/10.1007/978-3-319-30634-6_4.

(48) Rosner, B.; Glynn, R. J. Power and Sample Size Estimation for the Wilcoxon Rank Sum Test with Application to Comparisons of C Statistics from Alternative Prediction Models. *Biometrics* **2009**, *65* (1), 188–197. https://doi.org/10.1111/j.1541-0420.2008.01062.x.

(49) Posit team. RStudio: Integrated Development Environment for R, 2025. http://www.posit.co/.

(50) Ahmed, W.; Bertsch, P. M.; Bivins, A.; Bibby, K.; Farkas, K.; Gathercole, A.; Haramoto, E.; Gyawali, P.; Korajkic, A.; McMinn, B. R.; Mueller, J. F.; Simpson, S. L.; Smith, W. J. M.; Symonds, E. M.; Thomas, K. V.; Verhagen, R.; Kitajima, M. Comparison of Virus Concentration Methods for the RT-qPCR-Based Recovery of Murine Hepatitis Virus, a Surrogate for SARS-CoV-2 from Untreated Wastewater. *Sci. Total Environ.* **2020**, *739*, 139960. https://doi.org/10.1016/j.scitotenv.2020.139960.

(51) Philo, S. E.; Keim, E. K.; Swanstrom, R.; Ong, A. Q. W.; Burnor, E. A.; Kossik, A. L.; Harrison, J. C.; Demeke, B. A.; Zhou, N. A.; Beck, N. K.; Shirai, J. H.; Meschke, J. S. A Comparison of SARS-CoV-2 Wastewater Concentration Methods for Environmental Surveillance. *Sci. Total Environ.* **2021**, *760*, 144215. https://doi.org/10.1016/j.scitotenv.2020.144215.

(52) Bustin, S. A.; Benes, V.; Garson, J. A.; Hellemans, J.; Huggett, J.; Kubista, M.; Mueller, R.; Nolan, T.; Pfaffl, M. W.; Shipley, G. L.; Vandesompele, J.; Wittwer, C. T. The MIQE Guidelines: Minimum Information for Publication of Quantitative Real-Time PCR Experiments. *Clin. Chem.* **2009**, *55* (4), 611–622. https://doi.org/10.1373/clinchem.2008.112797.

(53) Taylor, S.; Wakem, M.; Dijkman, G.; Alsarraj, M.; Nguyen, M. A Practical Approach to RT-qPCR—Publishing Data That Conform to the MIQE Guidelines. *Methods* **2010**, *50* (4), S1–S5. https://doi.org/10.1016/j.ymeth.2010.01.005.

(54) Souza, R. R. de; Toebe, M.; Mello, A. C.; Bittencourt, K. C. Sample Size and Shapiro-Wilk Test: An Analysis for Soybean Grain Yield. *Eur. J. Agron.* **2023**, *142*, 126666. https://doi.org/10.1016/j.eja.2022.126666.

(55) Hauke, J.; Kossowski, T. Comparison of Values of Pearson's and Spearman's Correlation Coefficients on the Same Sets of Data. *Sciendo* **2011**. https://doi.org/10.2478/v10117-011-0021-1.

(56) Zheng, X.; Li, S.; Deng, Y.; Xu, X.; Ding, J.; Lau, F. T. K.; In Yau, C.; Poon, L. L. M.; Tun, H. M.; Zhang, T. Quantification of SARS-CoV-2 RNA in Wastewater Treatment Plants Mirrors the Pandemic Trend in Hong Kong. *Sci. Total Environ.* **2022**, *844*, 157121. https://doi.org/10.1016/j.scitotenv.2022.157121.

(57) Bivins, A.; Kaya, D.; Bibby, K.; Simpson, S. L.; Bustin, S. A.; Shanks, O. C.; Ahmed, W. Variability in RT-qPCR Assay Parameters Indicates Unreliable SARS-CoV-2 RNA

Quantification for Wastewater Surveillance. *Water Res.* **2021**, *203*, 117516. https://doi.org/10.1016/j.watres.2021.117516.

(58) Chomczynski, P.; Sacchi, N. The Single-Step Method of RNA Isolation by Acid Guanidinium Thiocyanate–Phenol–Chloroform Extraction: Twenty-Something Years On. *Nat. Protoc.* **2006**, *1* (2), 581–585. https://doi.org/10.1038/nprot.2006.83.

(59) Ma, W.; Wang, M.; Wang, Z.-Q.; Sun, L.; Graber, D.; Matthews, J.; Champlin, R.; Yi, Q.; Orlowski, R. Z.; Kwak, L. W.; Weber, D. M.; Thomas, S. K.; Shah, J.; Kornblau, S.; Davis, R. E. Effect of Long-Term Storage in TRIzol on Microarray-Based Gene Expression Profiling. *Cancer Epidemiol. Biomark. Prev. Publ. Am. Assoc. Cancer Res. Cosponsored Am. Soc. Prev. Oncol.* **2010**, *19* (10), 2445–2452. https://doi.org/10.1158/1055-9965.EPI-10-0565.

(60) Thatcher, S. A. DNA/RNA Preparation for Molecular Detection. *Clin. Chem.* **2015**, *61* (1), 89–99. https://doi.org/10.1373/clinchem.2014.221374.

(61) Schirtzinger, E. E.; Kim, Y.; Davis, A. S. Improving Human Coronavirus OC43 (HCoV-OC43) Research Comparability in Studies Using HCoV-OC43 as a Surrogate for SARS-CoV-2. *J. Virol. Methods* **2022**, *299*, 114317. https://doi.org/10.1016/j.jviromet.2021.114317.

(62) Pecson, B. M.; Darby, E.; Haas, C. N.; Amha, Y. M.; Bartolo, M.; Danielson, R.; Dearborn, Y.; Giovanni, G. D.; Ferguson, C.; Fevig, S.; Gaddis, E.; Gray, D.; Lukasik, G.; Mull, B.; Olivas, L.; Olivieri, A.; Qu, Y.; Consortium, S.-C.-2 I. Reproducibility and Sensitivity of 36 Methods to Quantify the SARS-CoV-2 Genetic Signal in Raw Wastewater: Findings from an Interlaboratory Methods Evaluation in the U.S. *Environ. Sci. Water Res. Technol.* **2021**, *7* (3), 504–520. https://doi.org/10.1039/D0EW00946F.

(63) Scott, G.; Evens, N.; Porter, J.; Walker, D. I. The Inhibition and Variability of Two Different RT-qPCR Assays Used for Quantifying SARS-CoV-2 RNA in Wastewater. *Food Environ. Virol.* **2023**, *15* (1), 71–81. https://doi.org/10.1007/s12560-022-09542-z.

(64) Hutchison, J. M.; Li, Z.; Chang, C.-N.; Hiripitiyage, Y.; Wittman, M.; Sturm, B. S. M. Improving Correlation of Wastewater SARS-CoV-2 Gene Copy Numbers with COVID-19 Public Health Cases Using Readily Available Biomarkers. *FEMS Microbes* **2022**, *3*, xtac010. https://doi.org/10.1093/femsmc/xtac010.

(65) Hsu, S.-Y.; Bayati, M.; Li, C.; Hsieh, H.-Y.; Belenchia, A.; Klutts, J.; Zemmer, S. A.; Reynolds, M.; Semkiw, E.; Johnson, H.-Y.; Foley, T.; Wieberg, C. G.; Wenzel, J.; Johnson, M. C.; Lin, C.-H. Biomarkers Selection for Population Normalization in SARS-CoV-2 Wastewater-Based Epidemiology. *Water Res.* **2022**, *223*, 118985. https://doi.org/10.1016/j.watres.2022.118985.

(66) Randazzo, W.; Truchado, P.; Cuevas-Ferrando, E.; Simón, P.; Allende, A.; Sánchez, G. SARS-CoV-2 RNA in Wastewater Anticipated COVID-19 Occurrence in a Low Prevalence Area. *Water Res.* **2020**, *181*, 115942. https://doi.org/10.1016/j.watres.2020.115942.

(67) Kuang, D.; Gao, X.; Du, N.; Huang, J.; Dai, Y.; Chen, Z.; Wang, Y.; Wang, C.; Lu, R. Wastewater Surveillance as a Predictive Tool for COVID-19: A Case Study in Chengdu. *PloS One* **2025**, *20* (5), e0324521. https://doi.org/10.1371/journal.pone.0324521.

(68) Gonzalez, R.; Curtis, K.; Bivins, A.; Bibby, K.; Weir, M. H.; Yetka, K.; Thompson, H.; Keeling, D.; Mitchell, J.; Gonzalez, D. COVID-19 Surveillance in Southeastern Virginia Using Wastewater-Based Epidemiology. *Water Res.* **2020**, *186*, 116296. https://doi.org/10.1016/j.watres.2020.116296.

(69) Cutrupi, F.; Rossi, M.; Cadonna, M.; Poznanski, E.; Manara, S.; Postinghel, M.; Palumbi, G.; Bellisomi, M.; Nicosia, E.; Allaria, G.; Dondero, L.; Veneri, C.; Mancini, P.; Ferraro, G. B.; Rosa, G.; Suffredini, E.; Foladori, P.; Grasselli, E. Evaluation of Concentration Procedures, Sample Pre-Treatment, and Storage Condition for the Detection of SARS-CoV-2 in Wastewater. *Environ. Sci. Pollut. Res.* **2023**, *30* (48), 106660–106670. https://doi.org/10.1007/s11356-023-29696-y.

(70) Kitajima, M.; Ahmed, W.; Bibby, K.; Carducci, A.; Gerba, C. P.; Hamilton, K. A.; Haramoto, E.; Rose, J. B. SARS-CoV-2 in Wastewater: State of the Knowledge and Research Needs. *Sci. Total Environ.* **2020**, *739*, 139076. https://doi.org/10.1016/j.scitotenv.2020.139076.

(71) Ahmed, W.; Bertsch, P. M.; Bibby, K.; Haramoto, E.; Hewitt, J.; Huygens, F.; Gyawali, P.; Korajkic, A.; Riddell, S.; Sherchan, S. P.; Simpson, S. L.; Sirikanchana, K.; Symonds, E. M.; Verhagen, R.; Vasan, S. S.; Kitajima, M.; Bivins, A. Decay of SARS-CoV-2 and Surrogate Murine Hepatitis Virus RNA in Untreated Wastewater to Inform Application in Wastewater-Based Epidemiology. *Environ. Res.* **2020**, *191*, 110092. https://doi.org/10.1016/j.envres.2020.110092.

(72) Maal-Bared, R.; Qiu, Y.; Li, Q.; Gao, T.; Hrudey, S. E.; Bhavanam, S.; Ruecker, N. J.; Ellehoj, E.; Lee, B. E.; Pang, X. Does Normalization of SARS-CoV-2 Concentrations by Pepper Mild Mottle Virus Improve Correlations and Lead Time between Wastewater Surveillance and Clinical Data in Alberta (Canada): Comparing Twelve SARS-CoV-2 Normalization Approaches. *Sci. Total Environ.* **2023**, *856*, 158964. https://doi.org/10.1016/j.scitotenv.2022.158964.

(73) Olesen, S. W.; Imakaev, M.; Duvallet, C. Making Waves: Defining the Lead Time of Wastewater-Based Epidemiology for COVID-19. *Water Res.* **2021**, *202*, 117433. https://doi.org/10.1016/j.watres.2021.117433.

(74) Cai, L.; Zhang, T. Detecting Human Bacterial Pathogens in Wastewater Treatment Plants by a High-Throughput Shotgun Sequencing Technique. *Environ. Sci. Technol.* **2013**, *47* (10), 5433–5441. https://doi.org/10.1021/es400275r.

(75) Philo, S. E.; De León, K. B.; Noble, R. T.; Zhou, N. A.; Alghafri, R.; Bar-Or, I.; Darling, A.; D'Souza, N.; Hachimi, O.; Kaya, D.; Kim, S.; Gaardbo Kuhn, K.; Layton, B. A.; Mansfeldt, C.; Oceguera, B.; Radniecki, T. S.; Ram, J. L.; Saunders, L. P.; Shrestha, A.; Stadler, L. B.; Steele, J. A.; Stevenson, B. S.; Vogel, J. R.; Bibby, K.; Boehm, A. B.; Halden, R. U.; Delgado Vela, J. Wastewater Surveillance for Bacterial Targets: Current Challenges and Future Goals. *Appl. Environ. Microbiol. 90* (1), e01428-23. https://doi.org/10.1128/aem.01428-23.

(76) Barber, C.; Crank, K.; Papp, K.; Innes, G. K.; Schmitz, B. W.; Chavez, J.; Rossi, A.; Gerrity, D. Community-Scale Wastewater Surveillance of Candida Auris during an Ongoing Outbreak in Southern Nevada. *Environ. Sci. Technol.* **2023**, *57* (4), 1755–1763. https://doi.org/10.1021/acs.est.2c07763.

(77) Baker, T.; Bester, P. A.; Sebolai, O. M.; Albertyn, J.; Pohl, C. H. Culture-Dependent and -Independent Wastewater Surveillance for Multiple Pathogenic Yeasts. *J. Fungi* **2025**, *11* (2), 86. https://doi.org/10.3390/jof11020086.

(78) Quintero-Betancourt, W.; Gennaccaro, A. L.; Scott, T. M.; Rose, J. B. Assessment of Methods for Detection of Infectious Cryptosporidium Oocysts and Giardia Cysts in Reclaimed Effluents. *Appl. Environ. Microbiol.* **2003**, *69* (9), 5380–5388. https://doi.org/10.1128/AEM.69.9.5380-5388.2003.

(79) Puchades-Colera, P.; Girón-Guzmán, I.; Díaz-Reolid, A.; Sánchez, G.; Pérez-Cataluña, A. Wastewater-Based Epidemiology for Waterborne Protozoa: A Comparison of Analytical Methods for Detecting *Cryptosporidium* Spp. *Sci. Total Environ.* **2025**, *987*, 179789. https://doi.org/10.1016/j.scitotenv.2025.179789.